2. DIFFRACTION GEOMETRY AND ITS PRACTICAL REALIZATION

cone. Generally, only a small fraction of this power is recorded by the detector. Thus, the useful quantity is the power per unit length of the diffraction circle on the receiving surface, $P'_\mathbf{h}$. At a distance r from the sample, the circumference of the diffraction circle is $2\pi r \sin 2\theta_0$ and one has (constants omitted)

$$P'_\mathbf{h} \propto r^{-1} V N_c^2 [i_0(E) j d^2 |F|^2]_\mathbf{h} \frac{C_p(E, \theta_0) \Delta\theta_0}{\sin\theta_0}. \qquad (2.5.1.7)$$

The peak areas in an XED powder spectrum are directly proportional to the $P'_\mathbf{h}$ of equation (2.5.1.7).

Quantitative structural analysis requires the knowledge of $i_0(E)$ and $P(E)$. As mentioned above, these quantities are not known with sufficient accuracy for *Bremsstrahlung*. For synchrotron radiation they can be calculated, but they will nevertheless contribute to the total uncertainty in the analysis. Accordingly, XED is used rather for identification of a known or assumed structure than for a full structure determination.

2.5.1.5. *Corrections*

(*a*) *Temperature effects*

The effect of thermal vibrations on the integrated intensities is expressed by the Debye–Waller factor in the same way as for standard angle-dispersive methods. Notice that $(\sin\theta)/\lambda = 1/2d$ irrespective of the method used. The contribution of the thermal diffuse scattering to the measured integrated intensities can be calculated if the elastic constants of the sample are known (Uno & Ishigaki 1975).

(*b*) *Absorption*

The transmission factor $A(E, \theta_0)$ for a small sample bathed in the incident beam and the factor $A_c(E, \theta_0)$ for a large sample intercepting the entire incident beam are the same as for monochromatic methods (Table 6.3.3.1). However, when they are applied to energy-dispersive techniques, one has to note that the absorption corrections are strongly varying with energy. In the special case of a symmetrical reflection where the incident and diffracted beams each make angles θ_0 with the face of a thick sample (powder or imperfect crystal), one has

$$A_c(E) = \frac{1}{2\mu(E)}, \qquad (2.5.1.8)$$

where $\mu(E)$ is the linear attentuation coefficient evaluated at the energy associated with the Bragg reflection.

(*c*) *Extinction and dispersion*

Extinction and dispersion corrections are applied in the same way as for angle-dispersive monochromatic methods. However, in XED, the energy dependence of the corrections has to be taken into account.

(*d*) *Geometrical aberrations*

These are distortions and displacements of the line profile by features of the geometry of the apparatus. Axial aberrations as well as equatorial divergence contribute to the angular range $\Delta\theta_0$ of the Bragg reflections. There is a predominance of positive contributions to $\Delta\theta_0$, so that the diffraction maxima are slightly displaced to the low-energy side, and show more tailing on the low-energy side than the high-energy side (Wilson, 1973).

(*e*) *Physical aberrations*

Displacements due to the energy-dependent absorption and reflectivity of the sample tend to cancel each other if the incident intensity, $i_0(E)$, can be assumed to be constant within the energy range of Bragg reflection. With synchrotron radiation, $i_0(E)$ varies rapidly with energy and its influence on the peak positions should be checked. Also, the detector response function will influence the line profile. Low-energy line shapes are particularly sensitive to the deadlayer absorption, which may cause tailing on the low-energy side of the peak. Integrated intensities, measured as peak areas in the diffraction spectrum, have to be corrected for detector efficiency and intensity losses due to escape peaks.

2.5.1.6. *The Rietveld method*

The Rietveld method (see Chapter 8.6) for refining structural variables has only recently been applied to energy-dispersive powder data. The ability to analyse diffraction patterns with overlapping Bragg peaks is particularly important for a low-resolution technique, such as XED (Glazer, Hidaka & Bordas, 1978; Buras, Gerward, Glazer, Hidaka & Olsen, 1979; Neuling & Holzapfel, 1992). In this section, it is assumed that the diffraction peaks are Gaussian in energy. It then follows from equation (2.5.1.7) that the measured profile y_i of the reflection k at energy E_i corresponding to the ith channel of the multichannel analyser can be written

$$y_i = \frac{c'}{H_k} i_0(E_i) A(E_i) j_k d_k^2 |F_k|^2 \exp\{-4\ln 2[(E_k - E_i)^2 / H_k^2]\},$$
$$(2.5.1.9)$$

where c' is a constant, $i_0(E_i)$ is evaluated at the energy E_i, and H_k is the full width (in energy) at half-maximum of the diffraction peak. $A(E_i)$ is a factor that accounts for the absorption in the sample and elsewhere in the beam path. The number of overlapping peaks can be determined on the basis of their position and half-width. The full width at half-maximum can be expressed as a linear function of energy:

$$H_k = UE_k + V, \qquad (2.5.1.10)$$

where U and V are the half-width parameters.

2.5.1.7. *Single-crystal diffraction*

Energy-dispersive diffraction is mainly used for powdered crystals. However, it can also be applied to single-crystal diffraction.

A two-circle system for single-crystal diffraction in a diamond-anvil high-pressure cell with a polychromatic, synchrotron X-ray beam has been devised by Mao, Jephcoat, Hemley, Finger, Zha, Hazen & Cox (1988).

Formulae for single-crystal integrated intensities are well known from the classical Laue method. Adaptations to energy-dispersive work have been made by Buras, Olsen, Gerward, Selsmark & Lindegaard-Andersen (1975).

2.5.1.8. *Applications*

The unique features of energy-dispersive diffraction make it a complement to rather than a substitute for monochromatic angle-dispersive diffraction. Both techniques yield quantitative structural information, although XED is seldom used for a full structure determination. Because of the fixed geometry, energy-dispersive methods are particularly suited to *in situ* studies of samples in special environments, *e.g.* at high or low temperature and/or high pressure. The study of anomalous scattering and forbidden reflections is facilitated by the possibility of shifting the diffraction peaks on the energy scale by changing the scattering angle. Other applications are studies of Debye–Waller factors, determinative mineralogy, attenuation-coefficient measurements, on-stream measurements, particle-size and -strain

determination, and texture studies. These and other applications can be found in an annotated bibliography covering the period 1968–1978 (Laine & Lähteenmäki, 1980). The short counting time and the simultaneous recording of the diffraction spectrum permit the study of the kinetics of structural transformations in time frames of a few seconds or minutes.

Energy-dispersive powder diffraction has proved to be of great value for high-pressure structural studies in conjunction with synchrotron radiation. The brightness of the radiation source and the efficiency of the detector system permit the recording of a diffraction spectrum with satisfactory counting statistics in a reasonable time (100–1000 s) in spite of the extremely small sample volume (10^{-3}–10^{-5} mm^3). Reviews have been given by Buras & Gerward (1989) and Häusermann (1992). Recently, XED experiments have been performed at pressures above 400 GPa, and pressures near 1 TPa may be attainable in the near future (Ruoff, 1992). At this point, it should be mentioned that XED methods have limited resolution and generally give unreliable peak intensities. The situation has been transformed recently by the introduction of the image-plate area detector, which allows angle-dispersive, monochromatic methods to be used with greatly improved resolution and powder averaging (Nelmes & McMahon, 1994, and references therein).

2.5.2. White-beam and time-of-flight neutron diffraction (By J. D. Jorgensen, W. I. F. David, and B. T. M. Willis)

2.5.2.1. *Neutron single-crystal Laue diffraction*

In traditional neutron-diffraction experiments, using a continuous source of neutrons from a nuclear reactor, a narrow wavelength band is selected from the wide spectrum of neutrons emerging from a moderator within the reactor. This monochromatization process is extremely inefficient in the utilization of the available neutron flux. If the requirement of discriminating between different orders of reflection is relaxed, then the entire white beam can be employed to contribute to the diffraction pattern and the count-rate may increase by several orders of magnitude. Further, by recording the scattered neutrons on photographic film or with a position-sensitive detector, it is possible to probe simultaneously many points in reciprocal space.

If the experiment is performed using a pulsed neutron beam, the different orders of a given reflection may be separated from one another by time-of-flight analysis. Consider a short polychromatic burst of neutrons produced within a moderator. The subsequent times-of-flight, t, of neutrons with differing wavelengths, λ, measured over a total flight path, L, may be discriminated one from another through the de Broglie relationship:

$$m_n(L/t) = h/\lambda, \qquad (2.5.2.1)$$

where m_n is the neutron mass and h is Planck's constant. Expressing t in microseconds, L in metres and λ in Å, equation (2.5.2.1) becomes

$$t = 252.7784 \, L\lambda.$$

Inserting Bragg's law, $\lambda = 2(d/n)\sin\theta$, for the nth order of a fundamental reflection with spacing d in Å gives

$$t = (505.5568/n)Ld\sin\theta. \qquad (2.5.2.2)$$

Different orders may be measured simply by recording the time taken, following the release of the initial pulse from the moderator, for the neutron to travel to the sample and then to the detector.
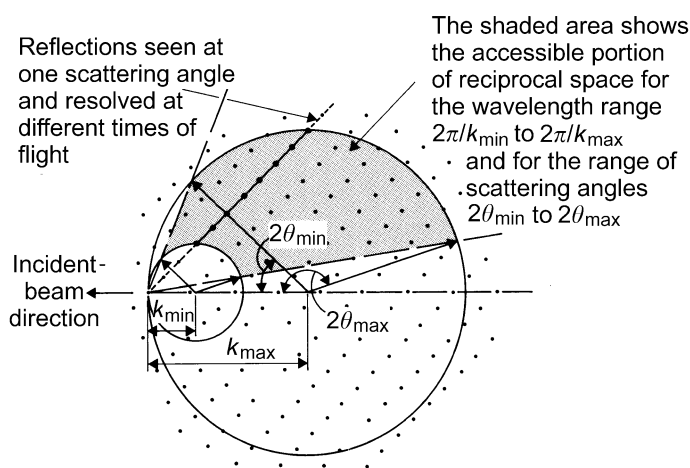

Fig. 2.5.2.1. Construction in reciprocal space to illustrate the use of multi-wavelength radiation in single-crystal diffraction. The circles with radii $k_{max} = 2\pi/\lambda_{min}$ and $k_{min} = 2\pi/\lambda_{max}$ are drawn through the origin. All reciprocal-lattice points within the shaded area may be sampled by a linear position-sensitive detector spanning the scattering angles from $2\theta_{min}$ to $2\theta_{max}$. With a position-sensitive area detector, a three-dimensional portion of reciprocal space may be examined (after Schultz, Srinivasan, Teller, Williams & Lukehart, 1984).

The origins of pulsed neutron diffraction can be traced back to the work of Lowde (1956) and of Buras, Mikke, Lebech & Leciejewicz (1965). Later developments are described by Turberfield (1970) and Windsor (1981). Although a pulsed beam may be produced at a nuclear reactor using a chopper, the major developments in pulsed neutron diffraction have been associated with pulsed sources derived from particle accelerators. Spallation neutron sources, which are based on proton synchrotrons, allow optimal use of the Laue method because the pulse duration and pulse repetition rate can be matched to the experimental requirements. The neutron Laue method is particularly useful for examining crystals in special environments, where the incident and scattered radiations must penetrate heat shields or other window materials. [A good example is the study of the incommensurate structure of α-uranium at low temperature (Marmeggi & Delapalme, 1980).]

A typical time-of-flight single-crystal instrument has a large area detector. For a given setting of detector and sample, a three-dimensional region is viewed in reciprocal space, as shown in Fig. 2.5.2.1. Thus, many Bragg reflections can be measured at the same time. For an ideally imperfect crystal, with volume V_s and unit-cell volume v_c, the number of neutrons of wavelength λ reflected at Bragg angle θ by the planes with structure factor F is given by

$$N = i_0(\lambda)\lambda^4 V_s F^2/(2v_c^2 \sin^2\theta), \qquad (2.5.2.3)$$

where $i_0(\lambda)$ is the number of incident neutrons per unit wavelength interval. In practice, the intensity in equation (2.5.2.3) must be corrected for wavelength-dependent factors, such as detector efficiency, sample absorption and extinction, and the contribution of thermal diffuse scattering. Jauch, Schultz & Schneider (1988) have shown that accurate structural data can be obtained using the single-crystal time-of-flight method despite the complexity of these wavelength-dependent corrections.

2.5.2.2. *Neutron time-of-flight powder diffraction*

This technique, first developed by Buras & Leciejewicz (1964), has made a unique impact in the study of powders in confined environments such as high-pressure cells (Jorgensen &

references